Lasers in Manufacturing Conference 2015

Measurement of the laser cut front geometry

Oliver Bocksrocker[a,b,c], Peter Berger[a*], Tim Hesse[c], Meiko Boley[a], Thomas Graf[a]

[a]*Institut für Strahlwerkzeuge (IFSW), Pfaffenwaldring 43, 70569 Stuttgart, Germany*
[b]*Graduate School of Excellence advanced Manufacturing Engineering (GSaME), Universität Stuttgart, Nobelstr. 12, 70569 Stuttgart,Germany*
[c]*TRUMPF Werkzeugmaschinen GmbH + Co. KG, Johann-Maus-Straße 2, 71254 Ditzingen, Germany*

Abstract

Solid-state lasers at the wavelength of about 1 µm have gained a rapidly increasing importance in the last few years for cutting metal sheets. As known from numerous investigations, the spatial distribution of the absorbed laser power is a key factor for the efficiency and the quality of the cutting process. Therefore, the exact cut front geometry is one major input parameter in order to investigate the influence of the absorption process.
In the present paper, measurements of the cut front geometry while cutting mild steel will be presented. A novel monitoring system, a so called quotient goniometer, enables recording temporally and spatially resolved measurements of the cut front geometry. The quotient goniometer exploits the angular- and polarization-dependent thermal emission of hot surfaces in order to measure the angle of the cutting front. The study shows that the cut front has a characteristic, straight profile while cutting with standard parameters. In addition the dynamic behavior of the molten material can be visualized with the quotient goniometer. It will be shown, that there is a high fluctuation of the cut front profile near the bottom of the cut front, while the shape in the upper half of the cut front typically remains constant over time. The measurements are compared to longitudinal sections to investigate the cut front geometry in the cutting direction.

Keywords: laser cutting; cut front geometry; thermal radiation; polarization; process monitoring

1. Introduction

In the last few years an increase of laser power up to 8 kW with a good focusability boosted the range of applications of the solid-state lasers in the area of cutting steel metal sheets up to a thickness of 40 mm. Compared to CO_2 lasers, the beam guidance via optical fiber and the higher efficiency and beam quality of the laser source are advantageous. If mild steel is cut with oxygen as a cutting gas, both laser sources offer a comparable quality and cutting performance up to a thickness of 20 mm, Poprawe et al., 2010. This progress proves solid-state lasers to be an attractive alternative to CO_2 lasers, even with thick metal sheets.

The cut front geometry is mainly formed by its absorption behavior due to the polarization state, the intensity distribution and the wavelength of the laser beam, Mahrle et al., 2004. As the wavelength of 1 µm and the statistical polarization state of the laser radiation is given, the inclination angle of the cut front geometry is an important factor for the absorption. Petring et al., 2012, investigated the influence of multiple reflections in the cutting zone on the cut front geometry. It is emphasized that multiple reflections can destabilize the lower cutting zone.

Scintilla et al., 2012, focused on the geometry of the laser cut front while cutting with different laser wavelengths, 1 µm and 10 µm, in order to explain the different cut quality of the fusion cutting process with stainless steel using nitrogen as an inert gas. It is shown that the inclination angle in the lower part of the cut front is reduced if the velocity increases, while in the upper part the inclination angle almost remains constant at different cutting velocities. The simulation results of Petring et al., 2012, show a familiar behavior of the inclination angle if the velocity increases. It is shown that a change of parameters such as the velocity can cause a significant change of the cut front geometry.

When mild steel is cut with oxygen, the exothermic energy provides the cutting process with energy, which influences the temperature along the cut front, Powell et al., 2009. It seems likely that the oxidation process influences the geometry of the cut front in addition to the absorption mechanism.

The temporally and spatially resolved online-measurement of the cut front geometry offers information about the state of the process in order to investigate the absorption and oxidation mechanisms. The angular and polarization characteristics of the thermal emissions of hot surfaces can be used to measure their inclination angle as described by Weberpals et al., 2011. To the best of the author's knowledge, temporally and spatially resolved measurements of the cut front geometry based on this principle are now realized for the first time.

2. Theoretical Background: Thermal radiation

The model of a black body describes an ideal surface, which absorbs the total amount of incoming radiation. If the temperature of the ideal surface is higher than absolute zero, the surface emits thermal radiation with a spectral density $L_{\lambda,black}(\lambda, T)$ which depends only on the temperature T and the wavelength λ, as described by Planck´s law. The emissivity ($\varepsilon_{black} = 1$) of a black body constitutes the maximum and cannot be reached by real surfaces.

The emissivity of a real surface ε_{real} additionally depends on the surface conditions (roughness, oxidation), the material and the angle of radiation β. It is defined as the quotient of the spectral density of a real surface $L_{\lambda,real}(\lambda, T, \beta,$ surface condition, material) and a black body surface $L_{\lambda,black}(\lambda, T)$. Furthermore, the emissivity has different characteristics for parallel (p-) and perpendicular (s-) polarization components, when the direction of radiation is not perpendicular to the surface. The Fresnel equations describe the absorptivity depending on the angle of inclination and the state of polarization. Following Kirchhoff's law, the absorptivity of a surface equals its emissivity at thermal equilibrium, Baehr, 2010.

Fig. 1 a) shows the angular dependence of the emissivity for the two temperatures of 300 K and 1800 K. The Figures 1 b) and c) show that the influence of the temperature between 300 K and 1800 K is negligible for iron if the quotient of the p- and s- polarized components of the radiation, or its multiplicative inverse are considered.

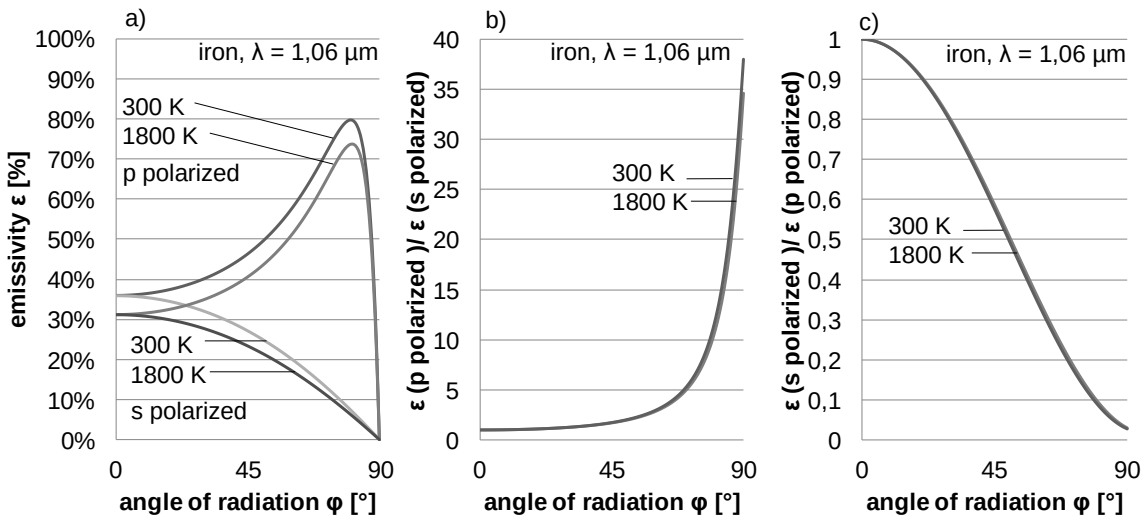

Fig. 1: Emissivity for p- and s-polarized radiation of iron at 300 K and 1800 K (a); quotient ε (p polarized) / ε (s polarized) (b); quotient ε (p polarized) / ε (s polarized) (c), values for n and k: Dausinger, 1995.

The Fresnel equations for the absorptivity of iron for radiation at parallel polarization and at perpendicular polarization are given by

$$A_P = \frac{4 \cdot n \cdot cos\varphi}{(n^2 + k^2) \cdot cos^2\varphi + 2 \cdot n \cdot cos\varphi + 1} \tag{1}$$

and

$$A_S = \frac{4 \cdot n \cdot cos\varphi}{n^2 + k^2 \cdot +2 \cdot n \cdot cos\varphi + cos^2\varphi} \tag{2}$$

respectively, where n and k are the refraction and extinction coefficients and φ is the angle of incidence on the irradiated surface, which is measured from the normal of the surface, Dausinger, 1995.

3. Experimental Setup

The scheme of the experimental setup is shown in Fig. 2. The laser light is transmitted through the dichroic mirror before it is focused onto the surface of the steel metal sheet. The thermal radiation of the cutting process is reflected by the dichroic mirror and transmitted into the quotient goniometer, which enables the separation of the p- and s-polarized components. The optical magnification is realized in two steps. A field diaphragm in the intermediate image plane of the thermal radiation provides a limitation of the image. The radiation is then collimated and transmitted into the beam splitter unit where it is split by two polarizers which are transmissive for s- and reflective for p-polarized radiation. The s- and the p- components are then imaged simultaneously on the same chip of an InGaAs-matrix detector with 320x256 pixels. The thermal radiation is filtered to a wavelength of 1600 ± 4 nm by the bandpass filter at the entrance of the

quotient goniometer. The two images are used to generate a quotient of both pictures. The images are recorded at a repetition rate of 80 Hz.

The experimental setup was first calibrated by mounting it on a robot system that allowed to tilt it in 5° steps, starting from 0° up to 80° (see Fig. 2, c). At each of these orientations the system was used to record the thermal radiation emitted from a plane surface of steel that was heated up to the melting point around 1800 K.

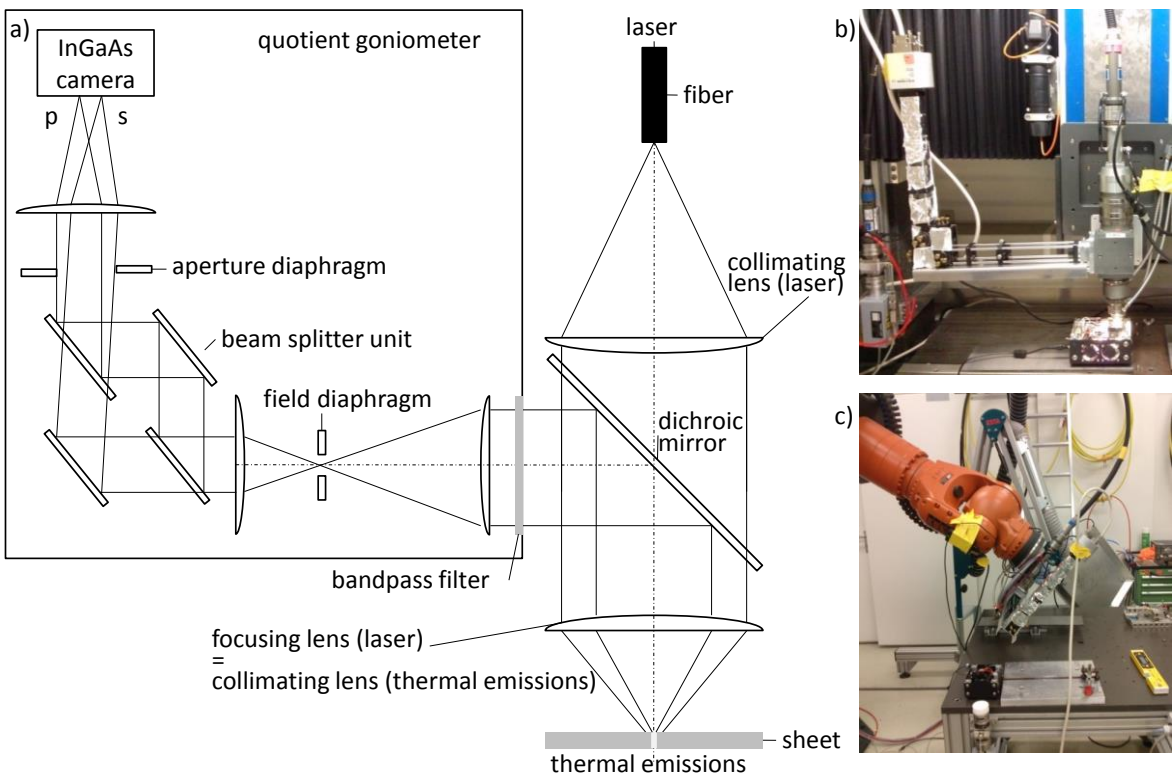

Fig. 2: Scheme of the experimental setup (a), laser cutting device (b), fixed on a robot for the calibration (c).

The measured values of the calibration are shown in Fig. 3 together with the fitted calibration function. As it is described above, the optical path and the characteristics of the dichroic mirror are different for the p- and s- components of the radiation. As a result the measured gray values of both images show a different intensity, even at a direction of radiation which is perpendicular to the surface. This leads to a quotient of the gray values s/p of around 40 % at an inclination angle of 0° in Fig. 3, compared to the theoretical value of 100 % in Fig. 1, c). The different intensities of the gray values of both images are also visible in Fig. 4 a) and b).

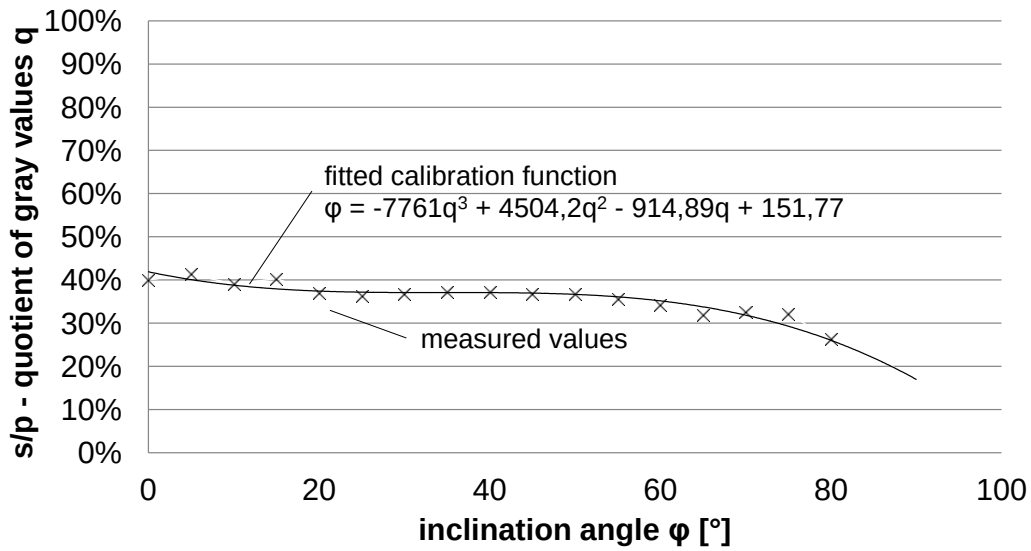

Fig. 3: Calibration: Measured values and the fitted calibration function of the inclination angle φ, where q is the quotient of the gray values s/p.

Fig. 4 shows the images of the p- (a) and s- (b) polarized components as well as the quotient p/s (c). The measuring line in the middle of the cutting gap points in cutting direction. The diagram in Fig. 4, d) shows the quotient of the gray values p/s as determined along the measuring line for one frame. For each pixel the above calibration function gives a calculated value of the inclination angle of the emitting surface.

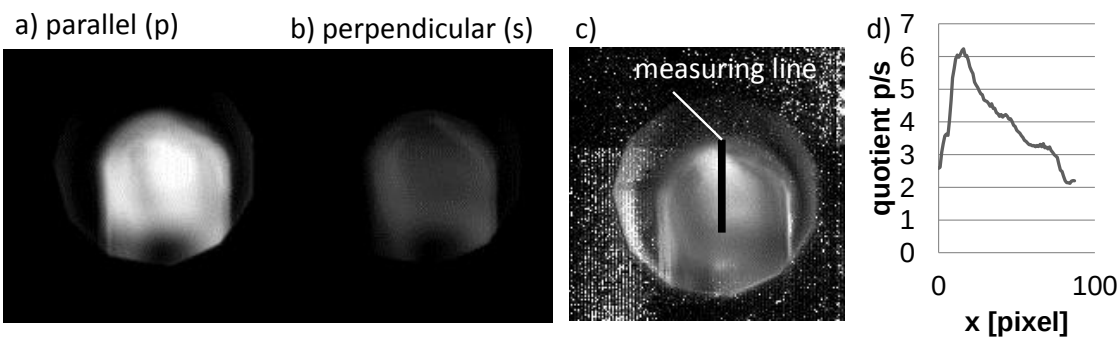

Fig. 4: Image of the p polarized component (a) and s polarized component (b), the quotient image p/s and the measuring line (c), the quotient of the gray values p/s (d).

4. Results

Temporally and spatially resolved measurements of the cut front geometry during oxygen cutting of 2 mm mild steel have been realized by means of the quotient goniometer described above. In a first experiment the cutting velocity was increased in constant increments of 0.4 m/min, while the other parameters were kept constant. In a second test, laser power was reduced in steps of 100 W until the cutting limit was

reached. In both processes the cutting limit was reached at the same energy per unit length of about 18 kJ/m.

To calculate the cut front geometry, the quotient of the gray values s/p is used to determine the inclination of the surface. This value can be integrated along the line measuring line can be integrated by using the angle distribution and the scale of the camera system. The extension in z-direction is reduced to values nearby 2 mm (sheet thickness) by modifying the fitted calibration function, in which the shape of the curve remains unchanged.

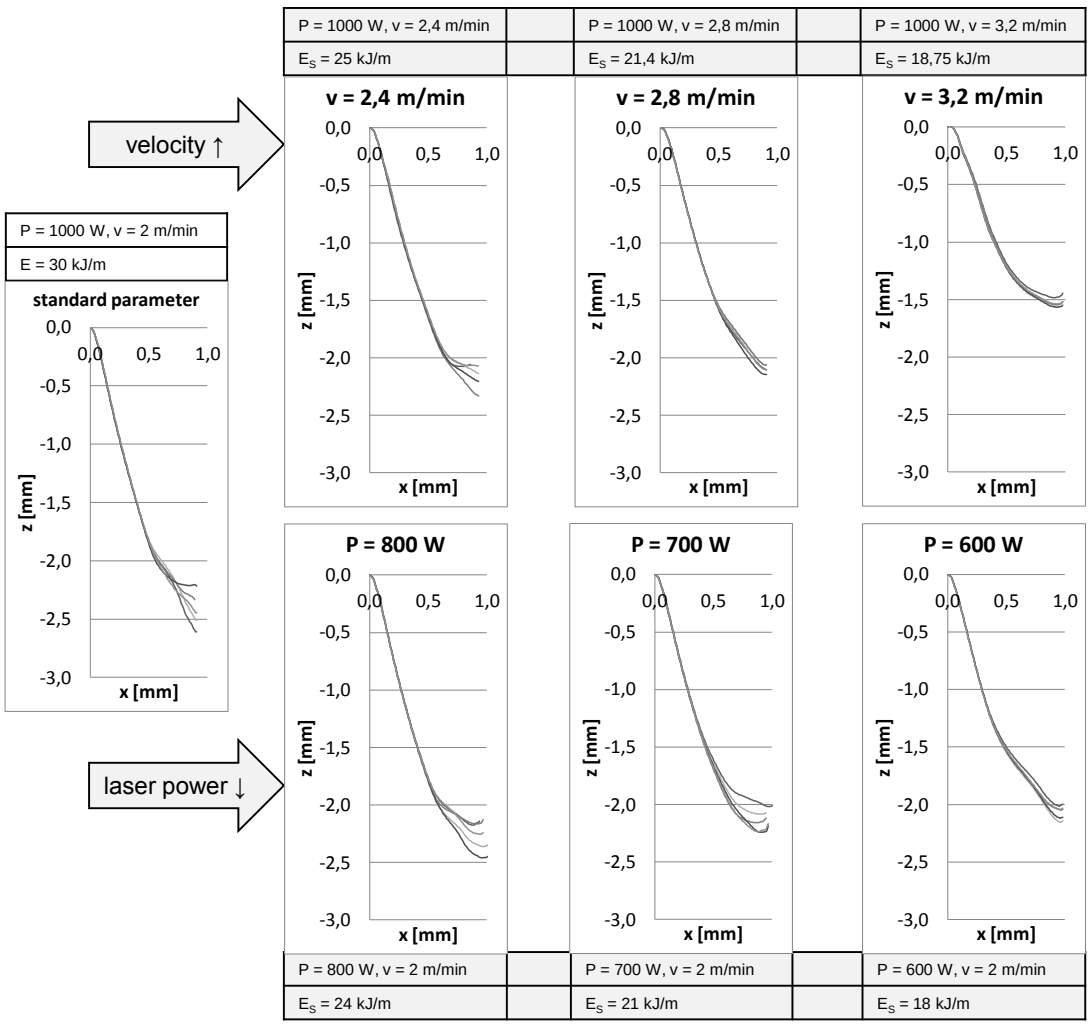

Fig. 5: Results of cutting 2 mm mild steel with the laser power P [W], the cutting velocity v [m/min] and the energy per unit length Es [kj/m].

The results are summarized in Fig. 5. Starting with standard parameters that result in a good surface quality of the cutting edge, the cut front geometry is mostly constant over time. Some minor fluctuations are visible in the lower part, which is assumed to be in the area of the melt expulsion. When only the energy per

unit length is reduced and all other parameters stay constant, the angle at z-positions of higher absolute values nearby 2 mm decreases continuously, while the inclination angle at lower absolute values of the z-position still stays almost constant. At high velocities, the cut front measurements show a shift of the lower inclination angles to z-positions with lower absolute values. As a result of the image limiting effect of the cutting nozzle, only the part at lower absolute values of the z-position is visible at high velocities.

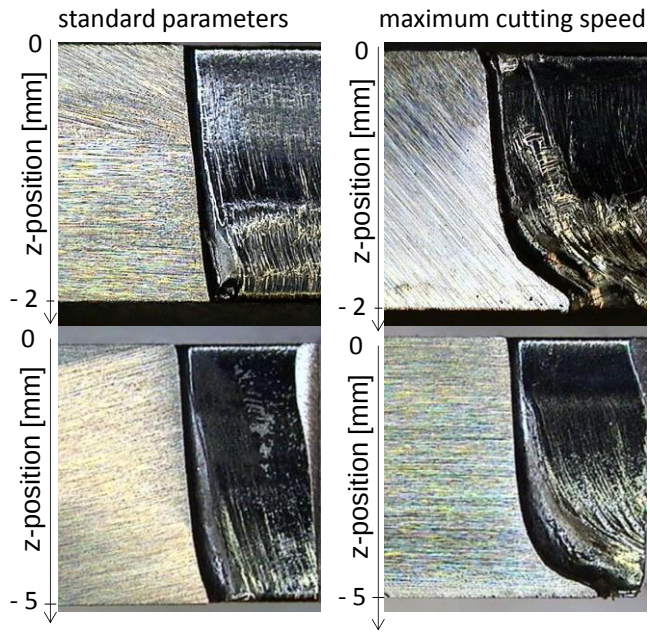

Fig. 6: Longitudinal sections of the cut front in 2 mm and 5 mm mild steel with standard parameters (left) and at the maximum cutting speed (right).

Using the angular- and polarization-dependent thermal emission, the measurements in 2 mm thick mild steel show a significant change of the cut front geometry, when the velocity is increased or the laser power is reduced. The measurements offer a similar shape of the cut front like the longitudinal sections in Fig. 6. It is shown, that the cut front geometry has a straight cut front, while cutting with standard parameters. A smaller inclination angle appears at z-positions of high absolute values (close to 2 mm) with an increase of velocity. This fits well to the online-measurements with the quotient goniometer.

5. Conclusion

The presented investigation show that the separation of the p- and s-polarized components of the thermal radiation emitted from the cutting front enables temporally and spatially resolved measurements of the angle of the cutting front, in order to investigate the geometry of the emitting surface. During reactive cutting of 2 mm thick mild steel, the measurements of the cut front geometry show a fluctuation of the angle of the lower part of the cut front, even when cutting with standard parameters. It seems likely that the fluctuations are caused by the melt expulsion at the bottom of the metal sheet while the cut front geometry itself has a temporally and spatially constant inclination angle. With an increase of the velocity or a decrease of the laser power, the cut front geometry changes predominately in the lower part of the cut front while in the upper part the inclination angle remains nearly constant over time.

Acknowledgements

The authors would like to thank the Graduate School of Excellence advanced Manufacturing Engineering (GSaME), Universität Stuttgart, which enabled the cooperation between the Institut für Strahlwerkzeuge (IFSW) and TRUMPF Werkzeugmaschinen GmbH + Co. KG.

References

Poprawe, R., Schulz, W., Schmitt, R., 2010. Hydrodynamics of material removal by melt expulsion: Perspectives of laser cutting and drilling, Physics Procedia 5, 1.

Mahrle, A., Beyer, E., 2009. Theoretical aspects of fibre laser cutting, J. Phys. D: Appl. Phys. 42, 175507

Petring, D., Molitor, T., Schneider, F., Wolf, N., 2012. Diagnostics, modeling and simulation: Three keys towards mastering the cutting process with fiber, disk and diode lasers, Physics Procedia 39, 186

Scintilla, L. D., Tricarico, L., Mahrle, A., Wetzig, A., Beyer, E., 2012. A comparative study of cut front profiles and absorptivity behavior for disk and CO2 laser beam, Journal of Laser Applications 24, 052006.

Powell, J., Petring, D., Kumar, R.V., Al-Mashikhi, S.O., Kaplan, A.F.H., Voisey, K.T., 2009. Laser–oxygen cutting of mild steel: the thermodynamics of the oxidation reaction, J. Phys. D: Appl. Phys. 42, 015504

Weberpals, J.-P., Berger, P., Graf, T., Trein, J., Singpiel, H., 2011. Novel Monitoring System For Spatially Resolved Topographical Measurement Of Laser-Based Processes, Proceedings of the Laser Materials Processing Conference (ICALEO) 204, 95

Baehr, H. D., Stephan, K., 2010. Wärme- und Stoffübertragung, Springer, Berlin, 627

Dausinger, F., 1995. Strahlwerkzeug Laser: Energieeinkopplung und Prozesseffektivität. B. G. Teubner-Verlag, Stuttgart, 74